0145–7632/01 $12.00 + .00

Analysis of Fouling in Refuse Waste Incinerators

M. C. VAN BEEK, C. C. M. RINDT, J. G. WIJERS, and A. A. VAN STEENHOVEN

Eindhoven University of Technology, Department of Mechanical Engineering, Eindhoven, The Netherlands

Gas-side fouling of waste-heat-recovery boilers, caused mainly by the deposition of particulate matter, reduces the heat transfer in the boiler. The fouling as observed on the tube bundles in the boiler of a Dutch refuse waste incinerator varied from thin and powdery for the economizer to thick and sintered for the superheater. Analysis of process data showed that both types of layers resulted in a 27% decrease of the heat transfer coefficient of the bundles.

To determine the important mechanisms in the deposition of particles, layers taken from the different bundles are analyzed using electron microscopy. The analysis revealed the existence of a melt in the thick deposit. The melt, giving rise to a liquid phase, increases the sticking efficiency of the deposit and leads to larger deposition rates. For the economizer and the superheater the actual deposition rate is calculated from the change in heat transfer. On the basis of a comparison between the calculated deposition rates and deposition rates to be expected in the case of a pure diffusion and thermophoresis process, it is shown that for both types of deposits inertia-controlled transport is the dominant transport mechanism of particles.

Steam-raising waste-heat-recovery boilers in refuse waste incinerators recover the useful energy content from the hot flue gases generated by combustion. These boilers are susceptible to fouling due to the presence of particulate matter (fly ash) and gaseous compounds in the flue gases. Fouling problems at the water/steam side are prevented by appropriate water treatment. Fouling, the formation of an insulating layer, reduces the overall heat transfer coefficient of the heat transfer surfaces and therefore the efficiency with which energy is recovered.

Flue gases are first cooled in the first draft of the boiler, where heat transfer is dominated by radiation. The fouling occurring in this part is usually referred to as slagging [1]. In the second draft, where flue gas temperatures are lower and heat transfer is due to convection, the flue gases are cooled using tube bundles placed in cross-flow with the flue gas flow. This study focuses on the fouling behavior of these tube bundles.

Insight into the relation between the geometry of the tube bundle and the formation of a fouling layer can be used to improve the performance of boilers that are susceptible to fouling. To develop a model that simulates the growth of a fouling layer as a function of geometry and process conditions, the important mechanisms responsible for the formation of a fouling layer need to be known.

The mechanism of fouling of heat transfer surfaces in a combustion environment is complex because it consists of condensation and chemical reaction in addition to particulation. Particulation, the deposition of particulate matter on the tubes in the boiler, is responsible for most of the deposited mass [2]. The deposition rate of particles is determined by the transport of particles to

The authors acknowledge the Centre of Sustainable Development at the Eindhoven University for funding this project and the refuse waste incinerators HVC in Alkmaar and AZN in Moerdijk for their contributions.

Address correspondence to Dr. Ir. C. C. M. Rindt, Department of Mechanical Engineering, section Energy-Technology, PO Box 513, 5600 MB, Eindhoven, The Netherlands. E-mail: C.C.M.Rindt@wtb.tue.nl

the surface and the sticking efficiency of these particles at the surface.

In the flue gases of a refuse waste incinerator, particles with sizes ranging from sub- to a few hundred micrometers are present. These particles are transported to the surface as a result of different phenomena. For submicrometer particles, transport is diffusion controlled. Due to the temperature gradient present, these particles in heat exchangers experience a force in the direction toward the cooler surface. This so-called thermophoretic effect augments the transport of sub- to a few-micrometers particles toward the heat exchange surface. The velocity with which these particles arrive at the surface is low, and, therefore, most of them are captured by the surface and stick. For particles larger than a few micrometers, inertia becomes important and the transport changes to inertia controlled. With this mechanism, transport rates are at least one order of magnitude larger than for diffusion and thermophoresis. The higher transport rates do not automatically result in higher deposition rates because the particles impact the surface with higher velocities. Therefore, not all the particles stick; some experience a rebound. The sticking efficiency in this case is a function of the kind of layer already deposited and increases strongly when a liquid phase appears at the surface of the deposit or on the particle itself.

In this article, the fouling taking place in the boiler of a refuse waste incinerator is analyzed. The analysis is focused on the kind of layers that appear in the boiler, their influence on the performance of the boiler, and the mechanisms that control the deposition of particulate matter on the tube bundles in the boiler. These mechanisms are derived by comparing the deposition rates calculated in this study from a measured decrease in heat transfer with deposition rates reported in other studies under different conditions.

PLANT DESCRIPTION

The fouling of the tube bundles in the boiler of a refuse waste incinerator is analyzed for two Dutch refuse waste incinerators. The two installations, located in Moerdijk and Alkmaar, fire refuse waste from households and companies and together generate the equivalent electricity use of 200,000 households. The steam-generating boilers in both installations operate under comparable conditions and have a similar design, given schematically in Figure 1, with a vertical first draft equipped with membrane walls and a horizontal second draft with tube bundles placed in the flue gas stream. In the second draft a mechanical cleaning system is installed. This system consists of hammers that periodically strike the hanging tube bundles. In Table 1 the specifications of the installation in Alkmaar are given.

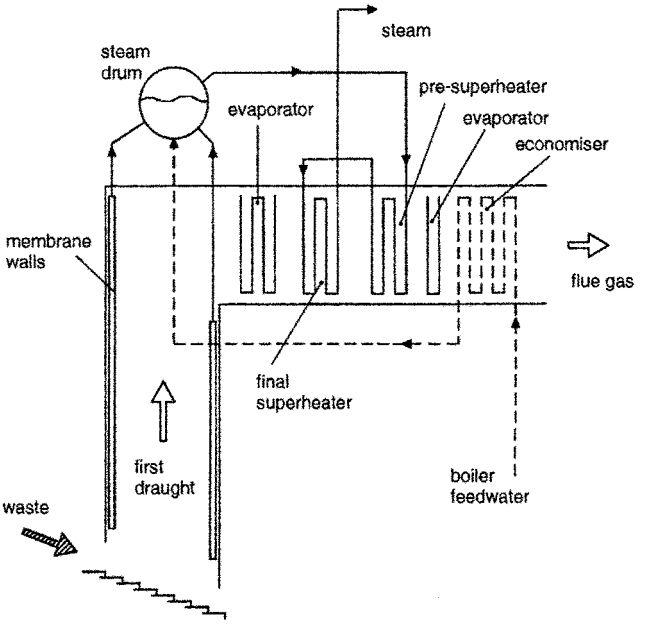

Figure 1 System layout of the boiler in Alkmaar.

In the boilers, water is first preheated in the economizers, after which it is fed to the steam drum. Next, steam is raised in the evaporators and superheated in the pre- and final super-heaters.

The fouling was visually examined during a boiler shutdown of the refuse waste incinerators in Alkmaar

Table 1 System's specifications of installation in Alkmaar; Reynolds number based on flue gas velocity and final superheater conditions

Boiler specifications		
Type	Double draft	
Steam		
Production	17	kg/s
Pressure	40	bar
Temperature	400	°C
Flue gas temperatures		
End of first draft	830	°C
Before final superheater	580	°C
Before economizer	340	°C
Boiler outlet	200	°C
Water/steam temperatures		
Boiler feed water	140	°C
Outlet economizer	212	°C
Entrance final superheater	335	°C
Flue gas velocity	5	m/s
Tube diameter	50	mm
Reynolds number	5,000	—
Tube materials		
Final superheater	15Mo3	
Economizer	St35-8	
Fly-ash concentration	4	g/kg

and Moerdijk. To analyze the structure and composition of the fouling layers, samples were taken of the layers that were still present on the tubes after the boiler had been taken offline. One sample was taken of the deposit on the final superheater and one of a powdery deposit such as had formed on the evaporator bundle prior to the economizer. The samples were analysed using XRD X-ray diffraction (XRD), electron-probe X-ray micro-analysis (EPXMA), and scanning electron microscopy (SEM).

Also, for the boiler in Alkmaar, process data were retrieved from the data management system to monitor the performance of the boiler. The variables were gathered as 4-h averages to ensure that short-time scale fluctuations, due to heterogeneity of the waste, are smoothed without losing too much information. The period for which the data were gathered was chosen around a plant shutdown during which the boiler was cleaned. In this way, the difference in performance of the boiler under clean and fouled conditions was obtained. For the gas side of the boiler, the flue gas temperatures in front of and behind the tube bundles were retrieved. For the water/steam side, the pressure and temperature at the inlet and outlet of each bundle was recorded together with the total flow rate of the water/steam.

LAYER ANALYSIS

From the visual examination, it appeared that the character of the fouling layer varied strongly as a function of local gas and tube temperatures. Large deposits were found on the final superheater, where the steam reaches its final temperature of 400°C, whereas the deposit on the economizer was thin and powdery.

The deposit on the final superheater, given schematically in Figure 2, consisted of a hard but brittle inner layer over the whole perimeter of the tube with a thickness of about 4 mm. This inner layer was lined at the tube side with a very thin corrosion layer. At the upstream side of the tube, on top of the inner layer, 2- to 3-cm-high gray-colored ridges had formed. The ridges were easily separable from the inner layer and crumbled off easily.

A sample taken from the deposit at the upstream side of a tube in the first row of the superheater tube bundle was analyzed to determine the structure and composition of the layer. In Figure 3, an overview is given of a cross section of the 4-mm-thick inner layer of this deposit, made using electron microscopy. The cross section shows a regular pattern of alternating compact and coarser structured and porous sublayers that are both about 0.5 mm thick. The coarse-structured layer consists of particles with sizes ranging from 5 to 30 μm that

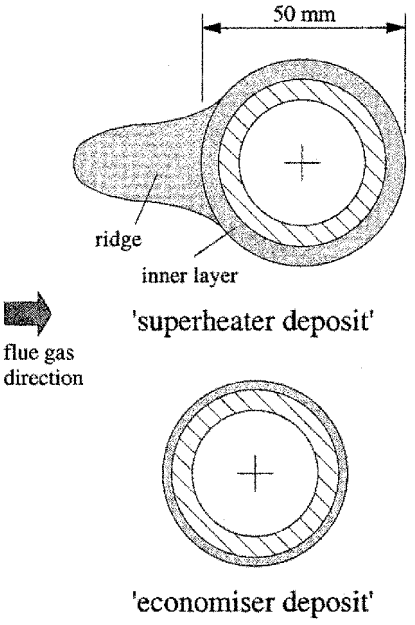

Figure 2 Main features of economizer and superheater deposits.

are embedded in a matrix material. The matrix, built of particles with sizes of the order of 1 μm consists from sulfates of sodium, potassium, and zinc, probably in a mixed compound with silica because this element was also detected homogeneously over the deposit. The elements detected by EPXMA correspond with the elements found in an XRD analysis of a ground sample of the deposit: Na, Al, Si, S, Cl, K, Ca, Fe, Zn, and Pb.

The compact layer is composed of the same fine-structured matrix with particle inclusions up to 30 μm. Within this matrix, local structures are found with sizes

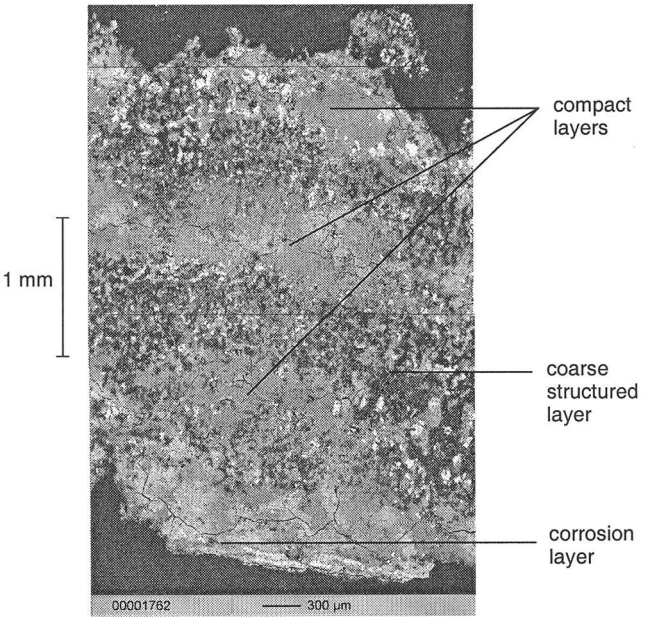

Figure 3 Cross section of the inner layer found on the final superheater tubes of the boiler in Moerdijk.

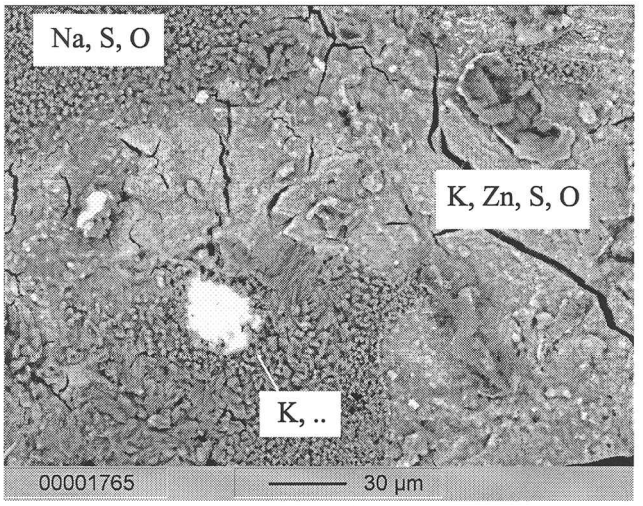

Figure 4 Element distribution in local structure.

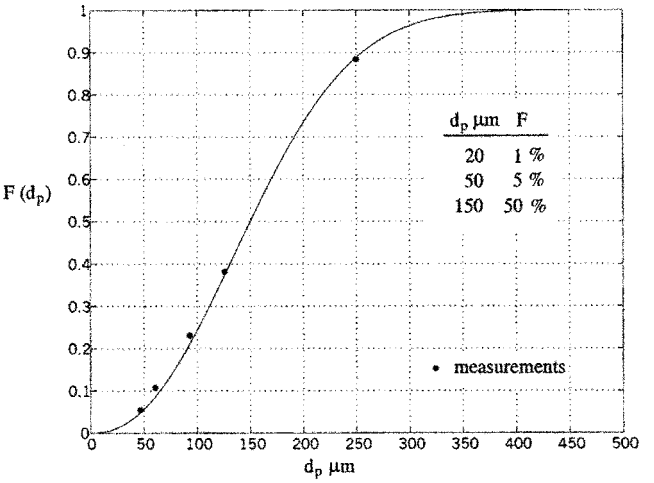

Figure 5 Fly-ash size distribution as measured for the boiler in Moerdijk.

much larger than that of the particles present. In these structures, there appeared to be a clear separation between the detected elements, as indicated in Figure 4.

In the case of formation of a melt in a multicomponent system, it is possible that different phases separate. Therefore, the detected distribution in elements over the local structure in the sample of the superheater deposit indicates the formation of a melt in the deposit. The formation of a melt in deposits taken from refuse waste incinerators was also demonstrated by Kerekes [3]. Kerekes reported peaks in the thermographs made of these deposits in the temperature range between 400 and 450°C, that is, just above the tube temperatures occurring in the final superheater. These temperatures were found to coincide with melting points of the binary system $Na_2SO_4 \cdot ZnSO_4$ and the tertiary system $Na_2SO_4 \cdot ZnSO_4 \cdot K_2SO_4$. The elements in these systems correspond with the detected elements over the structure as given in Figure 4.

The formation of a melt in the superheater deposit probably also explains the layered structure of the deposit. This is true because the formation of a melt results in a higher thermal conductivity of the layer, which, in turn, leads to a lower surface temperature. The surface temperature then becomes lower than the critical temperature for melting to occur, and the layer solidifies. Further deposition, however, makes the surface temperature increase again and the process repeats itself.

On the tubes of the economizer, a thin, white, and powdery layer had formed. The layer, only a few millimeters thick, is very soft and weak, such that upon the slightest contact the layer is removed. It should be noted that despite the layer's weakness, the layer was not removed by the mechanical cleaning system installed in the boiler. The deposit found on the evaporator bundle, prior to the economizer, has the same character as on the economizer except that the layer is somewhat stronger, which made it possible to take a sample that could be used for electron microscopy. The sample was taken from the upstream side of a cylinder positioned in the last row of tubes in the evaporator bundle.

Pictures taken of a cross section showed a porous, fine-structured layer consisting of particles of 1 to 10 µm. The absence of larger particles in the deposit indicates that the powdery layer has a limited sticking efficiency compared to that of the superheater deposit. This is in agreement with the appearance of a liquid phase in the layer of the superheater.

For both analyzed deposits the particle sizes observed represent only a small fraction of the particle sizes in the fly ash. The size distribution of the fly ash was measured using a sample taken from the boiler in Moerdijk. The cumulative mass distribution of the fly ash is given in Figure 5. The fly-ash sample was collected at the bottom of the boiler and was analyzed using standard sieves. The sampling position is likely to affect the measured distribution. However, because the measured distribution matches a distribution measured earlier for a Dutch refuse waste incinerator, it is regarded as representative for the size distribution in the boiler.

FOULING RESISTANCE

The influence of fouling on the performance is shown by monitoring the overall heat transfer coefficient of two bundles in the boiler. The decrease in heat transfer coefficient is expressed by the fouling resistance, which is later used to estimate the deposition rate. The heat transferred by a tube bundle is given by

$$Q = U_o A_o F \text{ LMTD} \quad (1)$$

with Q the heat transfer rate of the bundle, U_o the overall heat transfer coefficient, A_o the surface of the tube bundle, and LMTD the log mean temperature difference for the tube bundle multiplied by a correction factor F to account for the tube bundle not being an ideal parallel or counterflow heat exchanger. Because of the large number of passages over the bundle, this factor can be assumed to be unity [4]. From the retrieved process data, the overall heat transfer coefficient is calculated, using Eq. (1), for the 50-day period after the boiler had been cleaned by grid blasting. In this equation the heat transferred by the tube bundle, Q, is calculated using the measured steam flow rate. The LMTD is calculated using the inlet and outlet temperatures on the water/steam side and the flue gas temperatures measured in front of and behind the relevant tube bundle. The design values of these quantities are given in Table 1.

The fouling resistance, R_f, is used to express the decrease in the overall heat transfer coefficient, as given by

$$R_f = \frac{1}{U_o} - \frac{1}{U_{o,c}} \tag{2}$$

with $U_{o,c}$ the overall heat transfer coefficient under clean conditions that is observed directly after the boiler was cleaned. In Eq. (2) it is assumed that the heat transfer coefficient from the outer surface (either the tube wall or the surface of the fouling layer) to the flue gas flow is not affected by the formation of a deposition layer.

In Figures 6 and 7, the fouling resistance is shown as a function of time for the economizer and the final superheater tube bundle, respectively. It appears that both curves level off to an asymptotic value, implying that the heat transfer coefficient reaches a time-averaged constant value denoted with $U_{o,f}$. The asymptotic behavior is probably caused by the removal of deposited material due to erosion and fluid stresses. In addition, a changing surface temperature or a decrease in fly-ash concentration could have an effect. An increasing surface temperature reduces the transport by thermophoresis but enhances the sticking efficiency when melting is induced, thereby increasing the deposition rate. So, when assuming that inertia and not thermophoresis dominates the transport of fly ash to the tubes, an increasing surface temperature cannot explain the observed asymptote. Because no significant decrease in the amount of fly ash was seen over time, the latter possibility is also disregarded. The fouling curve can be approximated by

$$R_f = R_{f,\infty}(1 - e^{-t/\kappa}) \tag{3}$$

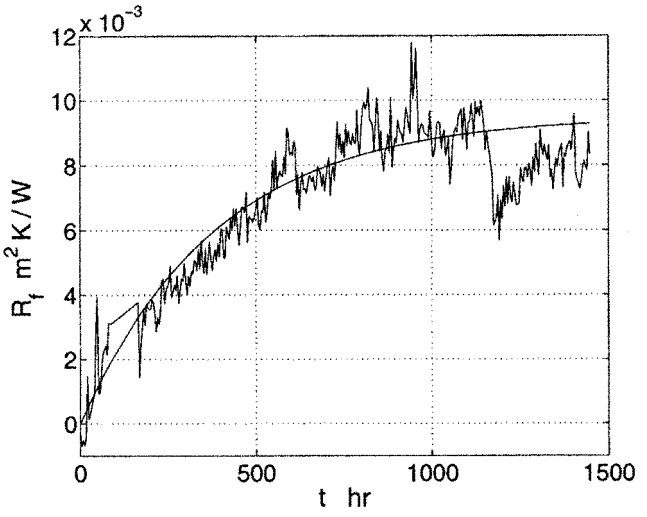

Figure 6 Fouling resistance economizer bundle of the boiler in Alkmaar.

with $R_{f,\infty}$ the asymptotic value and κ the time constant, which is defined as

$$\kappa = \frac{R_{f,\infty}}{(dR_f/dt)|_{t=0}} \tag{4}$$

The asymptotic value is found by substituting $U_{o,f}$ for U_o in Eq. (2). The time constant is found by curve-fitting the fouling resistance. Both quantities are given in Table 2, together with the initial and the final overall heat transfer coefficient for the economizer and superheater tube bundle.

From Table 2, it appears that fouling for both the economizer and the final superheater results in a decrease in the overall heat transfer coefficient of about 27%. This implies that the thin and powdery layer found on the economizer has the same relative influence on the

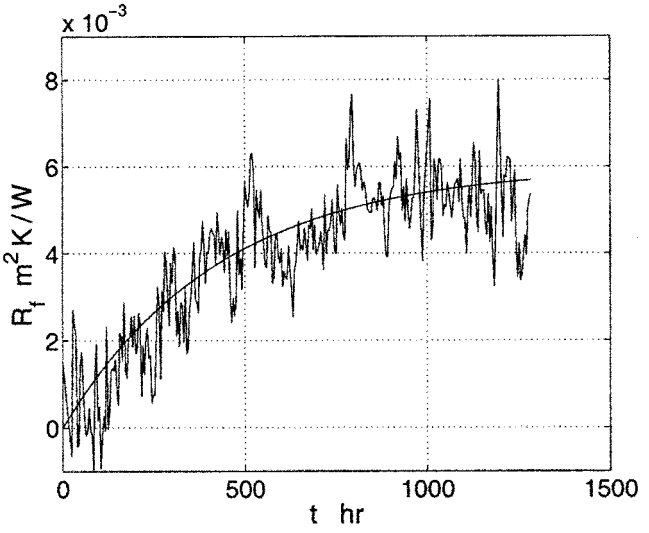

Figure 7 Fouling resistance final superheater bundle of the boiler in Alkmaar.

Table 2 Fouling resistance

Tube bank	$U_{o,c}$ (W/m^2 K)	$U_{o,f}$ (W/m^2 K)	$R_{f,\infty}$ (m^2 K/W)	κ (h)
Economizer	41 ± 5	30 ± 5	0.009 ± 0.001	380 ± 10
Final superheater	65 ± 5	45 ± 5	0.006 ± 0.001	430 ± 10

Table 3 Layer properties and deposition rate

Tube bank	$\lambda_{f,\infty}$ (mm)	$k_{f,\infty}$ (W/m K)	ρ_f (kg/m^3)	ϕ_d (kg/m^2 s)
Economizer	1	0.1	1,300	9×10^{-7}
Final superheater	4	0.7	1,900	5×10^{-6}

heat transfer coefficient as the thick and sintered deposit formed on the tubes of the superheater bundle. The large influence of the thin powdery layer implies that the thermal conductivity of this layer is much smaller than that of the superheater deposit.

DEPOSITION RATE

The calculated fouling curves are used to estimate the deposition rate for both the economizer and the superheater. Knowledge about this deposition rate is important because it gives information about the controlling mechanisms in the deposition of particulate matter in a refuse waste incinerator. Assuming the influence of the curvature to be negligible, the fouling resistance is determined by

$$R_f = \frac{\lambda_f}{k_f} \tag{5}$$

The change in thickness of the layer, λ_f, can be written as the net result of deposition and removal divided by the effective density of the deposited material:

$$\frac{d\lambda_f}{dt} = \frac{\phi_d - \phi_r}{\rho_f} \tag{6}$$

where ϕ_d and ϕ_r are, respectively, the deposition and removal rates in mass per unit time and per unit area, and ρ_f is the effective density of the deposited material that is a function of the porosity of the deposit. Following Kern and Seaton [5] asymptotic behavior as defined in Eq. (3) is found for the fouling resistance when it is assumed that the deposition rate is constant and the removal rate is proportional to the thickness of the layer already deposited. In that case, initially the removal rate is negligible and the initial change of the fouling resistance can be written as

$$\left.\frac{dR_f}{dt}\right|_{t=0} = \frac{\phi_d}{\rho_f k_f} \tag{7}$$

from which, using the definition for the time constant given in Eq. (4), the deposition rate can be derived:

$$\phi_d = \frac{\rho_f k_f R_{f,\infty}}{\kappa} \tag{8}$$

In the derivation of Eq. (8), it is assumed that the growth rate of the layer is constant over both the perimeter and along the length of the tube surface. The systematic error introduced is expected to be small because the thickness of the inner layer found on the superheater, as well as the powdery deposit, showed only a small nonuniformity.

To evaluate the deposition rate in addition to the already-known parameters from the fouling curve, the effective density and thermal conductivity of the deposit need to be known. Using Eq. (5), the characteristic thermal conductivity of both types of layers can be estimated from the calculated asymptotic heat transfer resistance and the observed layer thickness. The thermal conductivity of the powdery layer, given in Table 3, proves to be much smaller than that of the superheater deposit. Both conductivitie s correspond with the values reported by Raask [6], 0.1 W/m K for a powdery deposit, and 1 W/m K for a sintered deposit. The conductivitie s also agree with values found in thermal conductivity measurements for different slags by Wain et al. [7].

The effective density is estimated by weighing the different samples and measuring their volume and is also given in Table 3. The difference in density between the economizer and the superheater deposits is the result of a difference in porosity that is likely the result of melting in the superheater deposit.

The deposition rate found for the economizer, given in Table 3, is much smaller than that found for the superheater.

TRANSPORT MECHANISM

The deposition rate is a function of the particle sizes present in the flue gases that determine the controlling mode of transport. For small particles, roughly sub- to a few micrometers, transport is controlled by diffusion and thermophoresis, while for larger particles transport rates increase because inertia becomes important. A measure for the importance of the inertia of the particle is given by the particle relaxation time κ_p, the time scale in which a particle can adapt to a change in the fluid's velocity, which is defined by [8]

$$\kappa_p = \frac{\rho_p d_p^2}{18\eta_g} \tag{9}$$

with ρ_p the particle density, d_p the particle diameter, and η_g the dynamic viscosity of the gas. The particle size for which inertia starts to be important can be found by comparing the particle relaxation time with the smallest time scale of the flow, the Kolmogorov scale, κ_K. When the particle relaxation time becomes larger than the time scale of the largest motions, κ_L, particle transport is still inertia controlled, but it is usually referred to as impaction. For particles with a relaxation time between the smallest and the largest time scales, the particle is influenced by the turbulent eddies and transport is usually referred to as eddy impaction. The largest time scale, κ_L, and the Kolmogorov time scale, κ_K, are defined by [9]

$$\kappa_K = \sqrt{\frac{\nu_g L}{V^3}} \qquad \kappa_L = \frac{L}{V} \tag{10}$$

with L taken as half the tube diameter and V the mainstream velocity. For a Reynolds number of about 5,000, the Kolmogorov time scale is 1×10^{-4} s and the large time scale is 5×10^{-3} s. So, by substituting these values for κ_p in Eq. (9), it is found that inertia starts to be important in particle transport for particles of 4 μm and that transport changes to impaction for particles of 30 μm. Here, the particle density is taken as 2,600 kg/m^3 and the dynamic viscosity as 3×10^{-5} kg/ms.

Given the particle sizes found in both deposits, inertia-controlled transport is important for the growth of both layers. Because the particles found in the layers on the economizer and the superheater are all smaller than the critical diameter for impaction, transport is in the eddy-impaction regime.

To determine the relative importance of inertia-controlled transport compared to transport by diffusion and thermophoresis for the deposition at the economizers, the observed deposition rates for this tube bank are compared with the deposition rates measured by Mutsaers in a configuration where transport is due only to diffusion and thermophoresis. Mutsaers [10] measured the deposition of Na_2SO_4 dust particles on air-cooled cylindrical tubes in cross-flow with the flue gases. In the laboratory setup, the submicrometer particles were generated by adding an aspirated sodium sulfate solution to the propane–air mixture fed to the burner. At the upstream stagnation point of the cylinder, a deposition rate of 20 mg/min m^2 was found. As can be seen from Table 4, the conditions for the economizers are different from the conditions encountered in the experiments of Mutsaers. Therefore, to compare them, the results of Mutsaers have to be scaled to the conditions that apply for the economizers. The results are scaled using a modified Stanton relation that was also used by Mutsaers to predict his results. In this relation that is given by

$$\mathrm{St} = \frac{\phi_d}{C_{p,d} V_\infty} = \mathrm{St}_s \cdot f\left(\alpha_{T,w}, \frac{T_g - T_w}{T_w}, \ldots\right) \tag{11}$$

the standard Stanton number, St_s, is multiplied by a correction factor taking into account the influence of thermophoresis on the mass transfer to the cooler surface. This standard Stanton number is a function of the Reynolds and Schmidt numbers that characterize the flow. The correction factor, derived by Rosner [11], is a strong function of the thermal diffusion factor, $\alpha_{T,W}$, evaluated at the wall temperature. For Na_2SO_4 particles, this factor drops significantly below temperatures of about 250°C. For the economizer, the wall temperature is estimated from the average water temperature over the bundle. Because the wall temperature is only 170°C, the correction factor becomes 5, yielding a Stanton number for the scaled case of 6×10^{-5}. The deposition rate expected for the economizer due to the transport by diffusion and thermophoresis then becomes 6×10^{-9} kg/m^2 s. This value is found by multiplying the Stanton number with a particle concentration of 0.02 g/m^3 and a mainstream velocity of 5 m/s. The used particle concentration is based on the cumulative size distribution given in Figure 5, a cutoff diameter of 5 μm, and a fly-ash concentration of 4 g/kg. The calculated deposition rate is much smaller than the observed deposition rate for the economizer, which indicates that most of the deposited mass is due to inertia-controlled transport.

Table 4 Measured deposition rates as function of particle size and process conditions

Study	Re	d_p (μm)	$C_{p,d}$ (g/m^3)	T_g (°C)	T_w (°C)	ϕ_d (kg/m^2 s)	V_d (m/s)
This study; economizer	6,100	0.1–400	0.10[a]	280	170	9×10^{-7}	0.009
This study; final superheater	3,400	0.1–400	0.09[a]	500	400	5×10^{-6}	0.05
Mutsaers [10]: original data	87	0.12	0.14	477	241	3×10^{-7}	0.002
Mutsaers [10]: scaled data	6,100	0.12	0.02[a]	280	170	6×10^{-9}	0.0003

[a]The concentrations are based on the cumulative mass distribution curve for the fly ash in the waste incinerator as given in Figure 5 with a cutoff diameter of 50 μm for the economizers and the superheater, and 5 μm for the scaled data of Mutsaers.

STICKING EFFICIENCY

Particulate deposition is the combined effect of transport and sticking. The latter is a strong function of the local gas and tube temperatures. The effect of these conditions is shown in Table 5, where the measured deposition rates are compared with results reported in literature. Because the deposition rates can be expected to be proportional to the mass concentration of the particles, they are converted to characteristic deposition velocities (V_d) by dividing the deposition rate by the concentration ($C_{p,d}$). Because deposition rates are relatively small, it is assumed that the fly-ash concentration and size distribution are equal for both the superheater and the economizer.

Howarth et al. [12, 13] measured deposition rates using a fouling probe installed in a refuse waste incinerator plant at Toulon, France. The cylindrical fouling probe consisted of two halves with one sample at the upstream side and one downstream. Deposition rates were calculated from a change in weight of the sample over a period of a few hours; and for a few characteristic runs, the results for the deposition at the upstream side are given in Table 5. In the experiments of Howarth et al., the effective concentration for deposition is based on the size distribution of the fly ashes in the Dutch incinerator and is assumed to be 10% of the total dust concentration (2 g/m^3).

Deposition rates are reported by Wessel and Wagoner [14] for a subscale test furnace firing finely ground coal. Deposition was measured for an array of closely spaced air-cooled tubes. Particle sizes ranged from submicrometer up to 20 μm. In the experiments, the partially sintered deposition layer grew about 2 mm per hour. For the above studies, the conditions such as the particle sizes, local gas and tube temperatures (T_g and T_w), and the measured deposition rates are given in Table 5.

The deposition rates found for the economizer and those measured in run T-4-01 of Howarth, given in Table 5, are an order of magnitude smaller than the deposition rate for the superheater and run T-2-06. In view of the range of particle sizes present in the flue gases, the transport mechanism is expected to be the same in both cases. Therefore, the observed difference is probably caused by a difference in the sticking efficiency, which is a strong function of gas and wall temperatures. The enhanced sticking efficiency is usually associated with the existence of a liquid phase in the deposit that is confirmed by the analysis of the superheater deposit. The presence of a liquid phase increases the sticking efficiency, because a liquid bridge is formed in the impact of a particle with the layer. The energy required to rupture this bridge is higher than to overcome the adhesion force in a dry contact.

Even without the presence of a liquid phase, a layer is able to develop, as is observed for the economizers. The sticking efficiency in this case is determined by the different characteristics of a powdery layer compared to that of a bare surface. Initially, with a bare-tube surface, only the submicrometer particles can deposit to form an initial layer. It is only the submicrometer particles that can deposit because these particles, transported by diffusion and thermophoresis, deposit with modest velocities. Larger particles, transported to the surface because of their inertia, have too large impact velocities to deposit directly, and experience a rebound [15]. Because of the absence of a liquid phase, the particles have a weak adherence to each other, as well as to the tube wall, and are easy to remove. The formation of an initial layer is confirmed by Steadman [16]. For coal-fired boilers, he reported an initial layer with a thickness of tens to hundreds of micrometers, depending on the position on the tube. After the formation of an initial layer, incoming particles impact with a dusty layer that shows totally different material behavior than the clean tube wall. Because of this changed behavior, not only are the smallest particles able to stick, but also above-micrometer-sized particles, as is shown by the particle sizes found in the analysis of the economizer deposit. Smouse [17] found the same range of particle sizes in experiments on a simulated superheater tube using gas firing with Al_2O_3 particles, where the deposit contained particles up to 20 μm.

The deposition rate reported by Wessel and Wagoner is another order of magnitude larger than the deposition rate found for the superheater. The difference is thought to be the result of the particles becoming sticky, which is likely, considering the flue gas temperature in their

Table 5 Comparison of the measured deposition rates and deposition rates reported in the literature for comparable situations

Study	Re	d_p (μm)	T_g (°C)	T_w (°C)	ϕ_d (kg/m^2 s)	V_d (m/s)
This study; economizer	6,100	0.1–400	280	170	9×10^{-7}	0.009
This study; final superheater	3,400	0.1–400	500	400	5×10^{-6}	0.05
Wessel and Wagoner [14]	6,800	0.1–20	1,149	510	7×10^{-4}	1.3
Howarth: T-4-01 [12, 13]	4,200	0.1–100	393	182	1×10^{-6}	0.01
Howarth: T-2-06 [12, 13]	3,200	0.1–100	719	320	2×10^{-5}	0.2

installation of around 1,100°C. To prevent a fast-growing layer on the superheater because of these "sticky" particles, in the refuse waste incinerator, an additional evaporator bundle was placed before the superheater bundles to reduce the flue gas temperature at the entrance of the superheaters.

CONCLUSIONS

The character of the fouling layers developing on the tubes in the boiler of a refuse waste incinerator varies strongly over the different bundles. In the final superheater, a thick and sintered layer was found, and in the economizer only a thin, powdery layer had formed. From the analysis of process data, it was established that both type of layers resulted in a 27% drop in the overall heat transfer coefficient. The fact that the thin, powdery layer has such enormous consequences on the heat transfer coefficient arises from the nature of the deposit. The deposit is very fine structured and consists of particles ranging from sub- to supermicrometers, with a maximum of 10 μm. Such a fine-structured porous layer has a very low thermal conductivity. The thick and sintered deposit has a much higher thermal conductivity because of locally occurring melts in the deposit.

The appearance of a melt in the deposit was confirmed by the analysis of samples taken of deposits that had formed on the tubes in the boiler of a Dutch refuse waste incinerator. The appearance of a liquid phase, either by the formation of a melt in the deposit or by particles becoming sticky themselves, leads to larger deposition rates because of enhanced sticking efficiency of the particles. For the growth of a fouling layer on either the economizer or the superheater, the transport of these particles is mostly inertia controlled. The transport, however, is not in the pure impaction regime but rather in the "eddy impaction" regime.

To simulate the growth rate of a fouling layer by the deposition of particulate matter, both the transport and the sticking of particles need to be modeled. Because, for both the superheater and the economizer, most of the deposited mass is due to inertia-controlled transport, this type of transport needs to be incorporated into the deposition model. For particles of a few micrometers and larger, the sticking efficiency cannot be assumed to be unified and, to predict deposition rates accurately, a reliable model for the sticking efficiency is required. A model based on the assumption that the impact of a particle with the surface can be modeled as a two-body collision and the particle has to overcome a certain energy barrier for a rebound seems appropriate for this purpose [18]. Because no experiments are available to verify the assumptions made in the various models, an experimental apparatus was designed and built [19], with which the sticking efficiency for various surfaces can be measured. In the experiments, first, the sticking efficiency of a powdery deposit will be examined.

NOMENCLATURE

A_o	tube bundle surface area, m^2
C_p	particle concentration, kg/m^3
d_p	particle diameter, m
D_{cyl}	cylinder diameter, m
F	correction factor
k	thermal conductivity, W/m K
L	length scale, m
LMTD	log mean temperature difference, K
Q	heat transfer rate, W
R_f	fouling resistance, m^2 K/W
Re	Reynolds number
St	Stanton number
Stk	Stokes number
t	time, s
T	temperature, K
V_d	deposition velocity, m/s
U_o	overall heat transfer coefficient, W/m^2 K
V	velocity, m/s
V_∞	mainstream velocity, m/s
α	thermal diffusion factor
ε	porosity
η	dynamic viscosity, kg/m s
λ	thickness, m
ν	kinematic viscosity, m^2/s
ρ	density, kg/m^3
κ	time constant, s
ϕ	mass flux, kg/m^2 s

Subscripts

c	clean
d	deposition
f	fouling layer
g	gas
K	Kolmogorov
L	length scale
o	outer surface
p	particle
r	removal
s	standard
T	temperature
w	wall
∞	asymptotic value

REFERENCES

[1] Bryers, R. W., Fireside Slagging, Fouling, and High-Temperature Corrosion of Heat-Transfer Surfaces Due to Impurities in Steam-Raising Fuels, *Prog. Energy Combustion Sci.*, vol. 22, pp. 29–120, 1996.

[2] Marner, W. J., Progress in Gas-Side Fouling of Heat-Transfer Surfaces, *Appl. Mech. Rev.*, vol. 43, no. 1, pp. 37–66, 1990.

[3] Kerekes, Z. E., Bryers, R. W., and Sauer, A. R., The Influence of Heavy Metals Pb and Zn on Corrosion and Deposits in Refuse-Fired Steam Generators, in R. W. Bryers (ed.), *Ash Deposits and Corrosion Due to Impurities in Combustion Gases*, pp. 455–472, Hemisphere, New York, 1978.

[4] *VDI-Wärmteatlas*, 7. Auflage, VDI-Verlag, Düsseldorf, 1994.

[5] Kern, D. Q., and Seaton, R. E., A Theoretical Analysis of Thermal Surface Fouling, *Br. Chem. Eng.*, vol. 4, no. 5, pp. 258–262, 1959.

[6] Raask, E., *Mineral Impurities in Coal Combustion*, Hemisphere, New York, 1985.

[7] Wain, S. E., Livingston, W. R., Sanyal, A., and Williamson, J., Thermal and Mechanical Properties of Boiler Slags of Relevance to Sootblowing, in S.A. Benson (ed.), *Inorganic Transformations and Ash Deposition during Combustion*, pp. 459–470, ASME, New York, 1991.

[8] Stock, D. E., Particle Dispersion in Flowing Gases, *J. Fluids Eng.*, vol. 118, pp. 4–17, 1996.

[9] Lesieur, M., *Turbulence in Fluids*, Kluwer, Dordrecht, the Netherlands, 1990.

[10] Mutsaers, P. L. M., Beerkens, R. G. C., and de Waal, H., Fouling of Heat Exchanger Surfaces by Dust Particles from Flue gases of Glass Furnaces, *Glastech. Ber.*, vol. 62, no. 8, pp. 266–272, 1989.

[11] Rosner, D. E., Thermal (Soret) Diffusion Effects on Interfacial Mass Transport Rates, *PhysicoChem. Hydrodynam.*, vol. 1, pp. 159–185, 1980.

[12] Glen, N. F., and Howarth, J. H., Modelling Refuse Waste Incineration Fouling, *2nd Natl. UK Heat Transfer Conf.*, vol. 1, pp. 401–420, 1988.

[13] Howarth, J. H., Seguin, P., Tabaries, F., and Osborn, G., Characterisation of Incineration Fouling, *Inst. Chem. Eng. Symp. Ser.*, vol. 2, no. 129, pp. 1029–1036, 1992.

[14] Wessel, R. A., and Wagoner, C. L., Ash Deposits—Initiating the Change from Empiricism to Generic Engineering Part 2: Initial Results, ASME Paper 86-JPGC-FACT-7, 1986.

[15] Rogers, D. E., and Reed, J., The Adhesion of Particles Undergoing an Elastic-Plastic Impact with a Surface, *J. Phys. D: Appl. Phys.*, vol. 17, pp. 677–689, 1984.

[16] Steadman, E. N., Erickson, T. A., and Folkedahl, B. C., Coal and Ash Characterization: Digital Image Analysis Applications, in S. A. Benson (ed.), *Inorganic Transformations and Ash Deposition during Combustion*, pp. 147–164, ASME, New York, 1991.

[17] Smouse, S. M., and Wagoner, C. L., Deposit Initiation via Thermophoresis: Part 2—Experimental Verification of Hypothesis Using a Simulated Superheater Tube, in S. A. Benson (ed.), *Inorganic Transformations and Ash Deposition during Combustion*, pp. 625–638, ASME, New York, 1991.

[18] Konstandopoulos, A. G., Effects of Particle Inertia on Aerosol Transport and Deposit Growth Dynamics, Ph.D. thesis, Yale University, New Haven, CT, 1991.

[19] Beek, M. C., Rindt, C. C. M., Wijers, J. G., and van Steenhoven, A. A., Experiments on the Sticking Behaviour of Particles Impacting a Fouled Surface, *Proc. 1998 AIChE Annual Meeting: Symp. on Advanced Technologies for Particle Processing*, Miami Beach, FL, vol. 1, pp. 343–348, 1998.

Marco van Beek is a Ph.D. student at the Eindhoven University of Technology, working on a joined project between the Departments of Mechanical and Chemical Engineering concerning the fouling of heat exchange equipment. In 1995, he received his M.Sc. degree in Mechanical Engineering from the same university. His graduation project concerned the design of a steam injection system for a laboratory gas-turbine set-up.

Camilo Rindt received his M.Sc. and Ph.D. degrees from Eindhoven University of Technology, the Netherlands. Until the end of 1990 he worked in the field of biomechanics. Since 1991 he has been a lecturer on thermal transport phenomena in the field of energy technology. His main interests are in the fields of conjugate heat transfer, radiation modeling, and fouling of heat exchangers. Regarding the latter topic, he is focusing on the fouling problems in waste incinerators and sugar plants.

Johan Wijers is an Associate Professor in Process Equipment Design in the Chemical Engineering Department of the Eindhoven University of Technology, where he received his M.Sc. degree in 1969. He has worked on design rules for heat transfer equipment such as cooling towers, scraped surface heat exchangers, and crystallizers. Recent research topics are membrane processes and precipitation reactors.

Anton van Steenhoven is a Professor of Energy Technology at the Department of Mechanical Engineering at the Eindhoven University of Technology. He gained his Ph.D. in 1979 on a thesis about the fluid mechanics of heart valves. His current research interests are the numerical and experimental analysis of fluid flow and heat transfer and its application to the design of energy equipment.